View metadata, citation and similar papers at core.ac.uk

brought to you by CORE

provided by Hal-Diderot

Mesenchymal stem cell delivery into rat infarcted myocardium using a porous polysaccharide-based scaffold: a quantitative comparison with endocardial injection.

Catherine Le Visage, Olivier Gournay, Najah Benguirat, Sofiane Hamidi, Laetitia Chaussumier, Nathalie Mougenot, James Flanders, Richard Isnard, Jean-Baptiste Michel, Stéphane Hatem, et al.

To cite this version:

Catherine Le Visage, Olivier Gournay, Najah Benguirat, Sofiane Hamidi, Laetitia Chaussumier, et al.. Mesenchymal stem cell delivery into rat infarcted myocardium using a porous polysaccharide-based scaffold: a quantitative comparison with endocardial injection.. Tissue Engineering: Parts A, B, and C, Mary Ann Liebert, 2012, 18 (1-2), pp.35-44. <10.1089/ten.TEA.2011.0053>. <inserm-00613948>

HAL Id: inserm-00613948

http://www.hal.inserm.fr/inserm-00613948

Submitted on 8 Aug 2011

HAL is a multi-disciplinary open access archive for the deposit and dissemination of scientific research documents, whether they are published or not. The documents may come from teaching and research institutions in France or abroad, or from public or private research centers.

L'archive ouverte pluridisciplinaire **HAL**, est destinée au dépôt et à la diffusion de documents scientifiques de niveau recherche, publiés ou non, émanant des établissements d'enseignement et de recherche français ou étrangers, des laboratoires publics ou privés.

MESENCHYMAL STEM CELL DELIVERY INTO RAT INFARCTED MYOCARDIUM USING A POROUS POLYSACCHARIDE-BASED SCAFFOLD: A QUANTITATIVE COMPARISON WITH ENDOCARDIAL INJECTION

Catherine Le Visage, Ph.D.,[a,*] Olivier Gournay, M.D.,[b] Najah Benguirat, M.D.[b] Sofiane Hamidi, M.Sc.,[a,c] Laeticia Chaussumier, M.Eng.,[c] Nathalie Mougenot, Ph.D.,[d] James A. Flanders, D.V.M,[e] Richard Isnard, M.D.,[b] Jean-Baptiste Michel, Ph.D.,[a] Stéphane Hatem, M.D., Ph.D.,[b] Didier Letourneur, Ph.D.,[a] Françoise Norol, M.D., Ph.D.,[c,f]

[a] Inserm, U698, Bio-ingénierie Cardiovasculaire, Hôpital Bichat, 46 Rue H. Huchard, F-75877 Paris Cedex 18, France.

[b] Inserm, UMRS 956, Faculté de Médecine Pierre-Marie Curie, 91 Boulevard de l'hôpital, F-75013 Paris, France

[c] Inserm, U790, Institut Gustave Roussy, 39, rue Camille Desmoulins, F-94805 Villejuif Cedex, France

[d] IFR14, PECMV, Université Pierre et Marie Curie, 105 boulevard de l'Hôpital, 75013 Paris

[e] Department Clinical Sciences, College of Veterinary Medicine, Cornell University, Ithaca NY 14853-6401, USA

[f] AP-HP, Biotherapy Unit, Hôpital de la Pitié Salpétrière, 83 Boulevard de l'hôpital, F-75013 Paris, France

* Corresponding author. Tel: +33 1.40.25.86.00; Fax: +33 1.40.25.86.02;

Email address: catherine.levisage@inserm.fr

ABSTRACT

The use of mesenchymal stem cells (MSCs) for tissue regeneration is often hampered by modest engraftment in host tissue. This study was designed to quantitatively compare MSCs engraftment rates after delivery using a polysaccharide-based porous scaffold or endocardial (EC) injection in a rat myocardial infarction model. Cellular engraftment was measured by quantitative RT-PCR using MSCs previously transduced with a lentiviral vector that expresses GFP. The use of a scaffold promoted local cellular engraftment and survival. The number of residual GFP^+ cells was greater with the scaffold than after EC injection (9.7% vs 5.1% at 1 month and 16.3% vs 6.1% at 2 months, respectively (n=5)). This concurred with a slight increase in mRNA VEGF level in the scaffold group ($p<0.05$). Clusters of GFP^+ cells were detected in the peri-infarct area, mainly phenotypically consistent with immature MSCs. Functional assessment by echocardiography at 2 months post infarct also showed a trend towards a lower left ventricular dilatation and a reduced fibrosis in the scaffold group in comparison to direct injection group (n=10). These findings demonstrate that using a porous biodegradable scaffold is a promising method to improve cell delivery and engraftment into damaged myocardium.

KEYWORDS

Mesenchymal stem cells, Heart, Polysaccharide, Scaffold, Transplantation, Myocardial infarction

INTRODUCTION

Ischemic injury induces a heart failure as the end of pathological remodelling of the myocardium. Conventional treatments do not replace lost cardiomyocytes, opening the way to new approaches such as genes, growth factors, and cell-based therapies.[1] Cardiac cell therapy has evolved quickly and a variety of candidate cells, mainly skeletal myoblasts, hematopoietic and more recently mesenchymal stem cells (MSCs) have been tested to repair damaged hearts. MSCs are an attractive cell source for therapeutic applications, particularly as they can be easily cultured and release a large array of soluble growths factors and cytokines underlying some paracrine effects.[2] Despite promising experimental studies and early clinical trials, up to now, progress in cell therapy is hampered by sub-optimal engraftment of donor cells into the myocardium.[3] Typical approaches to deliver MSCs to infarcted myocardium are intravenous (IV), intracoronary (IC) and endocardial (EC) injection.[4] In a quantitative study evaluating these three methods for MSC delivery in a porcine delivery, Freyman et al. reported an increased, but still limited, engraftment of MSCs after IC or EC injection when compared with IV infusion (3%, 6% and 0 %, respectively).[4] EC injection offers direct localization of cells to the injured area, but engraftment is limited by leakage out of the injection sites. IC delivery was associated with a high incidence of decreased coronary blood flow. More recently, in a canine acute myocardial ischemia model, Perin et al. found an increased vascularity and greater functional improvement with EC delivery than IC delivery of MSCs.[5]

The approach to improve exogenous cell delivery to tissue, whatever the cell source, is of major clinical importance and has stimulated further investigation on the use of bioengineered scaffolds as cell delivery vehicles.[6] One of the challenges involves the development of optimized biocompatible materials functioning as synthetic analogs of the extracellular matrix, that would both provide a substrate for transplanted cells and promote cell engraftment.[7] Many materials have been used including polyglycolic acid (PGA), collagen gel, alginate and gelatin mesh. In this context, we previously described the preparation of a polysaccharide-based scaffold as a novel biomaterial for cardiovascular engineering.[8] Naturally-derived polysaccharides are hydrophilic, biodegradable, biocompatible and can form highly hydrated gels that could mimick the extracellular matrix. [9]

Naturally-derived polysaccharides are hydrophilic, biodegradable, biocompatible and can form highly hydrated gels that could mimick the extracellular matrix.[9]

In the present study, we used a rat model of acute myocardial infarct to examine MSCs engraftment in infarcted tissue using this polysaccharide-based porous scaffold in comparison with endocardial injection. Syngeneic MSCs stably transduced with a lentiviral vector allowed accurate *in vivo* assessment of cell retention after cardiac delivery. The effects on cardiac remodelling and function were then evaluated.

MATERIAL AND METHODS

Culture, characterization and preparation of MSCs

MSCs were obtained from the bone marrow of syngeneic adult Lewis rats (Janvier). Briefly, cells were collected by flushing femurs and expanded in DMEM (Gibco) supplemented with 1% penicillin/streptomycin and 10% fetal bovine serum at 37°C in a 5% CO2 atmosphere. Cells were subcultured every 4-7 days.

Characterization of rat MSCs was performed by flow cytometry analysis with a phycoerythrin (PE)-conjugated anti-human CD45 (Immunotech) antibody (MoAb) (BioLegend) and with fluorescein isothiocyanate (FITC)-conjugated anti-CD90 (Becton Dickinson), anti-CD106 monoclonal and anti-CD29 MoAbs (BioLegend). MSCs were also characterized by their capacity to differentiate along adipogenic, chondrogenic, and osteogenic lineages.[10] The ability of MSCS to differentiate towards cardiac lineage is controversial. We did not obtain any cardiac differentiation from rat MSCs during our *in vitro* culture.

Scaffold preparation

Polysaccharide-based scaffolds were prepared using a mixture of pullulan (Hayashibara) and dextran (Pharmacia), and sodium carbonate was added as a porogen agent.[11] Chemical cross-linking was carried out using trisodium trimetaphosphate STMP (Sigma) under alkaline conditions as described.[12] After a freeze-drying step, a circular punch was used to cut 6mm diameter and 1mm thickness round-shaped porous scaffolds. Scaffolds were observed with Environmental Scanning Electron Microscopy (ESEM) using an ESEM-FEG (Philips XL 30, Netherlands) with an accelerating voltage of 15 kV at a pressure of 4 torrs. Fluorescent scaffolds were prepared by adding 1% of Fluorescein-IsoThioCyanate-dextran (Sigma) before cross-linking for confocal miscroscopy observation. Optical sections were acquired using a Zeiss LSM 510 confocal microscope (Carl Zeiss, Oberkochen, Germany), equipped with a 10x Plan-NeoFluar objective lens (numerical aperture of 0.3) (Carl Zeiss). FITC-dextran was excited at 488 nm with an argon laser and its fluorescent emission was

selected by a 505-530 nm bandpass filter. Scaffolds were submitted to UV prior to cell seeding. Cell loading was performed after cell trypsinization by rehydration of a dried scaffold with 20µL of cell suspension. In a first set of in vitro experiments, optimal cell density was determined using from $2x10^4$ to 10^6 cells/scaffold, with scaffold size ranging from 2mm to 10mm in diameter. A metabolic MTT assay was performed 1 day later, by incubating seeded scaffolds with 0.5 mg/mL of MTT (3-(4,5-dimethyldiazol-2-yl)-2,5 diphenyl tetrazolium bromide, Sigma) for 3 hours at 37°C. Resulting formazan crystals were solubilized in 0.5 mL of DMSO and absorbance was recorded at 570 nm with a microplate reader. Non-cellularized porous scaffolds were used as controls. Cell viability was assessed with a Live/dead kit (Invitrogen). Briefly, cellularized scaffolds were incubated with 4 µM calcein AM and 2 µM ethidium homodimer-1 solution (Invitrogen) for 1 hour at 37°C. Cellularized scaffolds were then observed with a Zeiss LSM 510 confocal microscope using a standard fluorescein bandpass filter for calcein and a propidium iodide filter for EthD-1.

Prior to in vivo administration, 10^6 cells were seeded on a 6mm porous scaffold with 20µL of cell suspension; thirty minutes after, once cells attached, scaffolds were placed in 1ml culture medium for complete rehydratation.

Animal study

Both the procedure and the animal treatment complied with the Principles of Laboratory Animal Care formulated by the National Society for Medical Research. The studies were carried out under authorization 006235 of the Ministere de l'Agriculture, France.

In a first set of 3 experiments, migration from scaffold to cardiac tissue was evaluated in healthy myocardium. Afterward, male syngenic Lewis rats were submitted to the ligation of the descending anterior left coronary artery. Fifteen minutes after infarct, rats received $1x10^6$ MSCs according to the following procedures: the endocardial (EC) group received 5 myocardial injections of MSCs suspended in 20µL of culture medium in the peri-infarct and infarct zones. In the patch group, the cellularized scaffold was covered by a clinical polytetrafluoroethylene (PTFE) membrane

(Pericardial, St Jude Medical) that was glued onto the infarcted area. For the control scaffold group, non-cellularized scaffolds were implanted in the same conditions.

Determination of cellular engraftment

For assessment of cell retention, Lewis rat MSCs were transduced using a lentiviral vectors construct consisting in a dual-promoter that included GFP under the regulation of the human EF1α promoter (EF1αGFP) and PAC under the human puromycin resistance gene (puromycin-N-acetyltransferase; PAC) promoter. Evaluation of the transduction efficiency was based on the percentage of GFP^+ cells. Three syngeneic lines of transfected MSC were thus obtained and mixed for *in vivo* administration (passages 4 to 9). Animals were randomly assigned to the delivery method, scaffold or EC group. Engraftment was evaluated 1 and 2 months following GFP^+ MSC delivery in the 2 groups (n=5 per group for each time point).

GFP+ cell quantification in cardiac tissue was performed using molecular analysis of gene expression by quantitative PCR. The heart was removed and infarct region, border zone and large area of peri-infarct healthy myocardium were cut into slices <0.5mm thick and immediately submerged in RNA later stabilization reagent (Sigma, France). A reference curve was established on the basis of the GFP expression level from defined numbers of GFP+ cells (triplicate samples from 10x103 to 1x106 GFP+ cells per sample) used as calibrator. Quantitative PCR was performed on a 7500 Real Time PCR System (Applied Biosystems) with standard cycling conditions. GFP expression levels were normalized relative to the expression of rat HPRT, UBC and Ywhaz. The number of residual GFP+ cells after EC injection or scaffold administration was estimated by report to the reference curve.

Histology, immunofluorescence and immunohistochemistry analysis

Analysis were performed after administration of GFP^+ MSCs or MSCs double labelled with thymidine analog 5-bromo-2'-deoxyuridine BrdU (10μM for 24 hours) and with a fluorescent dye (PKH26, Sigma) (n=3, each condition).

Left ventricles were harvested, fixed in buffered formalin and embedded in paraffin for histological stains or in OCT for cryosections and immunohistochemical study. Histological sections were stained with hematoxylin and eosin (H/E) and with Sirius red stain (0.1% in saturated picric acid solution). Fibrosis area and total ventricular area (LV) were quantified by histomorphometric measurement on Sirius red stained sections with Histolab software (Microvision). Fibrosis percentage was calculated as: (fibrosis area/total LV area) × 100.

Direct observation of PKH-labelled cells in myocardial tissue was performed on cryosections. Immunostaining of myocardial sections was performed using the primary antibodies, anti cardiac sarcomeric α-actinin (Sigma), anti-connexin-43 (Dako), anti-smooth muscle actin (Dako), anti-CD31 (Dako) and anti-GFP (Torrey Pines), secondary Alexa fluor goat anti-mouse 488 and 532 antibodies, all from Molecular Probes (Invitrogen) using a double-labelling technique. Immunostaining of BrdU-positive cells was performed by indirect immunohistochemistry with anti-BrdU mouse antibody (Calbiochem) and DAB staining. Sections were counterstained with haematoxylin before mounting.

Molecular analysis of gene expression by quantitative reverse transcription polymerase chain reaction (RT-PCR)

MMP-2, MMP-9 and VEGF expression were measured on infarcted heart administered with MSCs using scaffold or EC injection, 1 and 2 months after infarct, in comparison with control animals submitted to infarct without cell administration. Immediately after sacrifice, samples were fixed in RNA stabilization reagent (RNA Later, Sigma). All primers were designed using intron-flanking method. Quantitative PCR was performed on a 7500 Real Time PCR System (Applied Biosystems) with standard cycling conditions. For housekeeping gene selection, the stability of various reference genes was investigated from different samples of rat infarcted hearts. The expression stability of 7 commonly used reference housekeeping genes (GAPDH, 18S, ActB, CycA HPRT, UBCand YWHAZ) was analyzed using geNorm and expression stability was determined by the Genorm program. HPRT, UBC and YWHAZ were identified as most stable genes. Then, gene expression levels were normalized relatively to the expression of rat HPRT, UBC and Ywhaz. Quantification was

done with the Pfaffl's method.[13] Relative expression ratios were calculated by reporting values to those of the control animals.

Echocardiographic and catheterization protocols

For determination of cardiac function related to MSC delivery, non transduced MSCs were used. Animals were randomly assigned to the delivery method, either control, scaffold or EC group. All cardiac echocardiograms were recorded using an Acuson 128XP (Acuson corporation, Mountain View, California, USA) utilizing a 7-10Mhz transducer. The heart was first imaged in two-dimensional mode in the parasternal long axis and short axis views, to position the M mode cursor perpendicular to the interventricular septum and left ventricular posterior wall. Then, M mode images were obtained at a 100 mm/sec speed. At least 3 measurements of LV end-diastolic (LVEDD) and end-systolic diameters (LVESD) were selected and averaged from each animal and the analysis of contractile function was derived from the LV fractional shortening fraction (LVFS): (LVEDD-LVESD/LVEDD x 100). The echocardiographic examination was performed 7 days and 2 months after myocardial infarction by a blinded observer.

Statistics

All parameters were expressed as mean values ± standard deviation, except for engraftment results expressed as median values. A t-test was performed on fibrosis and mRNA data, a one way ANOVA test was performed on echocardiographic data and a two-way ANOVA was performed on engraftment data. Statistical significance level was set at 0.05.

RESULTS

Cellularized scaffold for implantation

We first examined the optimal conditions of MSCs seeding on the scaffold. Scaffolds from 2 mm to 50 mm in diameter could easily be obtained and a 6 mm diameter porous scaffold, suitable for the size of rat hearts, was chosen (Fig. 1A). Porosity of scaffolds was observed with Environmental Scanning Electron Microscopy (Fig. 1B). The use of FITC-labelled dextran into polysaccharide scaffolds allowed confocal laser scanning microscopy observation of the inner structure of hydrated scaffolds. A typical single optical slice of a porous scaffold is shown on Fig. 1C. A mean pore size of 195 µm and a porosity of 41% were calculated. Cells infiltrated very quickly (<1min) within the scaffold porous structure like in a sponge, and the maximum volume contained was 15 µL. Using a metabolic MTT assay at day 1, we confirmed that $2x10^4$ to 10^6 cells/scaffold could be seeded into 6 mm porous scaffold. Absorbance data as a function of the initial cell number is shown on Fig. 1D. Cells within the transparent scaffold could be observed with light microscopy as cell clusters (Fig. 1E). Cell viability at day 1 was demonstrated with a live & dead assay (Fig. 1F).

A first series of experiments was conducted with FITC-labelled non-cellularized scaffolds to determine the *in vivo* fate of porous scaffold in rat cardiac tissue (n=2). One month after implantation, scaffold was found intact on normal cardiac tissue (Fig. 2A, scaffold stained with alcian blue dye for imaging purposes), as confirmed by fluorescent microscopic observation of heart sections showing cardiac tissue green autofluorescence and FITC-labelled scaffold (Fig. 2B). In contrast, the scaffold on infarcted cardiac tissue was progressively degraded after implantation and only some remnants of the FITC-scaffold were seen embedded or integrated into the adjacent tissue on infarcted heart sections at 1 month (Fig. 2 C, D).

Engraftment of MSC

Typical MSCs were obtained and characterized by their spindle shaped morphology (Fig. 3A) and a $CD45^-CD90^+$, $CD45^-CD29^+$ and $CD45^-CD106^+$ phenotypic profile. From the third passage, $CD45^-CD90^+$ cells represented 93±3 % of the cultured cells (Fig. 3B). Additionally, under appropriate

inducing in vitro conditions, rat MSCs could display osteogenic, chondrogenic and adipogenic differentiation (Fig. 3C).

Quantification of cell engraftment into the infarcted heart was performed using MSCs transduced with a lentiviral vector that expresses eGFP (Fig. 3D). The transduction efficiency of MSCs assessed by FACS as a percentage of GFP^+ cells reached 98.8±2.5% (n=3). The number of residual $eGFP^+$ cells was estimated by quantitative RT-PCR, after calibration with defined numbers of sorted $eGFP^+$ MSCs (Fig. 3E). One month after administration of $1x10^6$ $eGFP^+$ MSCs, the median number of $eGFP^+$ cells in the myocardium was greater after administration using scaffold than following EC injection with respectively 9.7% and 5.1% of the administered cells in the myocardium (Table 1). Engraftment was confirmed at 2 months. The median number of $eGFP^+$ cells in the scaffold group and EC group represented 16% and 6.1% of the initial administered cells, respectively (n=5).

MSC localization

We then examined the ability of MSCs to migrate from the scaffold to the targeted tissue. MSCs localization was examined using $eGFP^+$ cells or cells double-labelled with a fluorescent dye PKH26 and BrdU (n=3). When cellularized scaffolds were implemented on healthy myocardium, no labelled cells were detected in cardiac tissue. On the contrary, one month after implantation of cellularized scaffold on injured myocardium (Fig. 4A), immunofluorescence staining detected numerous PKH-labelled cells in the thin peri-infarcted cardiac tissue (Fig. 4B); some BrdU-positive MSCs were also observed in the same border area (Fig. 4C). This suggested the influence of attractive signals from infarcted area to induce cells moving from the implanted scaffold towards the targeted area (Fig. 4D). These data were confirmed using $eGFP^+$ cells. In animals having MSCs implemented on scaffold, clusters of GFP^+ cells were clearly detected in the peri-infarct area and in bordering healthy myocardium, one month (n=3) and two months (n=3) post infarct (Fig. 4E) but no GFP^+ cells were detected within the infarct area. Most of the cells weakly co-expressed the CD106 marker indicating that the infused cells remained mainly phenotypically consistent with immature MSC cells (data not shown). Nevertheless, few cells expressed the cardiac tissue-specific marker, α-actinin (Fig. 4E) and connexin 43 (data not shown).

Ventricular remodelling and biochemical modifications after MSC delivery using scaffold or EC injection

It is believed that MSCs sustain the heart repair predominantly by facilitating endogenous processes, through paracrine effect particularly on scar formation and neovascularization. Haematoxylin and eosin (Fig. 5A, top row) and sirius red (Fig. 5A, bottom row) staining in histological heart sections were examined in animals having received cellularized scaffold or EC injection. Sirius red staining indicated collagen production into the infarcted area related to fibrosis. Quantitative measurement of fibrosis area on cardiac sections showed a trend, but not reaching significance, towards the reduction of fibrosis in the scaffold group compared to EC group (12±1% versus 16±3%, respectively) (Fig. 5B).

We also measured the local production of MMP-2 and MMP-9 using qRT-PCR. MMP-2 and MMP-9 mRNA per milligram of infarcted hearts were similar 1 and 2 months following MSC administration, whatever the delivery condition (not shown). In contrast, VEGF mRNA level was significantly higher 2 months after administration in the scaffold group (Fig. 5C, bottom row; $p<0.05$).

Echocardiographic and catheterism studies

Functional assessment by echocardiography was performed 7 days and 2 months after myocardial infarction and cardiac graft implantation. At the baseline (7th post-operative day) LVEDD, LVESD, and LVFS were similar in both EC (respectively 7.0±1; 5.5±1; 21.8±6.7; n=9) and scaffold groups (respectively 7.4±1.8; 5.4±1.8; 27±9.2; n=9) as in the control group having received non cellularized scaffolds (respectively 7.3±1.2; 5.2±1.4; 30.5±9.9; n=9). Progressive left ventricular dilatation and deterioration of LVFS were observed in the control group at 2 months. On the contrary, there was a trend towards a higher LVFS and a lower LVESD in the cellularized scaffold group at 2 months (Fig. 6).

DISCUSSION

The approach to administer stem cells for cell therapy is mainly dependent of our ability to safely ensure sufficient delivery of cells within the target tissue and adequate local engraftment and function at this site. Different delivery strategies are required with regard to delivered cell types. For cardiac tissue, the intramyocardial route is suited to large, adherent cells and has been safely used for MSC infusion but suffers of a low engraftment rate. The potential interest of scaffolds in cardiac cell therapy is increasingly investigated to repair damaged tissue.[14, 15] The use of cells in combination with appropriate scaffold should provide not only a physical support for cell orientation and proliferation but also molecular cues to direct cell survival, cell cycle progression, and the expression of different phenotypes.[16] In this context, cell-seeded biocompatible cardiac patches could be considered as a promising approach. This study was designed to evaluate quantitatively MSC delivery in ischemic myocardium using a 3D scaffold in comparison with endocardial injection. Using a novel chemical cross-linking process combined with a porogen agent, polysaccharide-based porous scaffolds were prepared. MSCs were seeded into this porous scaffold that supports rapid integration of seeded cells. The hydrogel structure would allow exchange of oxygen, nutrients, and metabolites inside the porous scaffold, as well as the diffusion of cells. We found that homing of MSCs from the scaffold to myocardium required a signal such as infarct remodelling. After 30 days, cell delivery was associated with a greater number of engrafted cells when compared to EC delivery, with about 10% of the initial seeded cells present in the scaffold group, in comparison with 5% following EC administration. This concurred with the MSC engraftment rate previously reported by Freyman et al after EC delivery in a porcine myocardial infarction model.[4] Differents factors could contribute to the improvement of cell delivery after implantation using a porous scaffold. A scaffold would provide a cell-friendly micro-environment as well as a substrate for the transplanted cells that would prevent cell loss.[17] It could also act as a mechanical support to enhance cell survival and cell proliferation. Indeed we observed an increase in GFP+ cell number from 1 month to 2 months after implantation, although this increase was not statistically significant. This suggests that a slight proliferation of implanted MSCs occurred.

Even if the mechanism of cardiovascular repair from adult stem cells remains highly unknown, it is believed that MSCs act through paracrine actions. In agreement, a significant, despite

modest, difference in the mRNA level of VEGF between scaffold and EC group was achieved here at 2 months, although no improved vascularization was evidenced (data not shown).

Quantitative analysis of engrafted cells was performed using GFP^+ transgenic cells. In comparison with engraftment assessment using immunohistochemical analysis that samples only a small fraction of the myocardium, this method enables the quantification of a low number of residual cells and their accurate detection through the entire myocardium. To our knowledge, this is the first time that cellular engraftment and survival in injured myocardium were measured by quantitative RT-PCR. Internalized iridium technique, as performed by Freyman et al., offers quite similar interest.[4] Overestimation linked to non specific labelling of macrophages after phagocytosis of dead cells can be excluded with this method. In contrast, underestimation could be related to a potential immune reaction to GFP^+ cells or to silencing of the GFP reporter gene during the process of differentiation, although these risks are not usually expected.[18, 19] The relationship between GFP quantification by RT-PCR and cell number was thus determined by analyzing heart samples with known number of cells.

Some experimental studies in large animal models and early clinical trial support the concept that MSCs improve heart function following myocardial infarction. Our seeded scaffold group demonstrated a trend towards an improvement of ventricular functions and fibrosis size. To expect better clinical effects, the number of seeded cells should be considered. Pouzet et al. have shown that there was a linear relationship between efficacy of functional improvement and the number of injected cells.[20] A recent study in a large animal model revealed evidence of a dose-response effect to the MSC therapy following surgical injection and only a high dose of $200x10^6$ MSCs reduced infarct size.[21] MSC delivery using the EC method is limited by the adverse events reported with high cell concentration and injection volume of 0.3 mL. In contrast, the initial number of cells can be easily increased using larger scaffolds; large porous scaffolds (2 cm in diameter) containing $200x10^6$ autologous bone marrow derived MSCs are currently implanted in a pig model of myocardial infarct. We are also conducting a dose-effect study with GFP^+ cells to evaluate the relative contribution of cell engraftment to functional recovery. At the moment, limited functional data with GFP labelled cells suggested that a residual number of $3x10^5$ MSC could sustained a regenerative effect.

PTFE membrane could be also involved in the lack of significant benefit in terms of functional improvement in animal receiving cellularized scaffold maintained using this membrane. Significant foreign body reaction and undesirable fibrous membrane with fibroblast proliferation has been reported using PTFE membrane; [22, 23] we observed by ourselves that membrane alone altered the epicardial anatomy. Control groups did not include the use of the PTFE membrane. At the time of the study, the membrane was the more convenient system to maintain our scaffold on the myocardial injury but we are now considering others devices.

Another approach is to construct 3D functional tissues by layering 2D cell sheets.[24, 25] This system allows for cell interconnection with gap junctions, resulting in electrically synchronous beating. Hamdi et al. recently compared such a bilayer myoblast cell sheet and a myoblast seeded collagen sponge.[26] In both cases, significant improvements in left ventricular ejection fraction (LVEF) compared with the controls were reported but could not be related to the detectable persistence of the myoblasts at the studied time point neither to an increased cytokine production. Residual cells were more abundant in the patch-treated hearts than in those covered with the myoblast sheets and the authors suggested that the benefits of cell transplantation could be potentiated by an epicardial deposition of a pre-shaped cellularized patch. In their study, the number of MSC at the time of delivery was not assessed since myoblast sheets production required 7 days of culture.[26] In another study, cells were embedded into a type I collagen matrix secured to heart with a fibrin sealant then cultured for 7 days. Despite high initial engraftment rates at 1 week, no hMSCs or residual patches were detectable at 4 weeks.[27] Addition of bioactive factors could modify the scaffold to specifically recruit stem cells in the cardiac injury site.[28] An injectable matrix metalloproteinase (MMP)-responsive, bioactive hydrogel was recently described as an *in situ* forming scaffold to deliver vascular cells derived from human embryonic stem cells (hESC).[29] Tissue-engineered cardiac grafts were also prepared by using various biomaterials such as small intestine submucosa (SIS) [30] and biodegradable porous alginate scaffolds, cultured for 4 to 7 days before implantation.[31] However, insufficient cell migration into scaffolds and inflammatory reaction due to scaffold biodegradation were reported. In comparison, our approach did not require any delay between seeding and implantation. Indeed, a fast infiltration of cells within the porous scaffold led to a cellularized patch

that could be implanted rapidly and seeded cells were thus evidenced here 1 and 2 months after scaffold implantation. A complete degradation of the scaffold was observed following implantation on infarcted tissue, but not on normal cardiac tissue. We have preliminary evidence of scaffolds degraded *in vitro* by leukocyte hydrolytic enzymes such as acid and alkaline phosphatase, as well as lysozyme, activities (unpublished results). Acid phosphatase and lysozyme have been shown to be more active in patients with acute myocardial infarction and might contribute to the in vivo degradation of scaffolds.[32] This complete degradation of the scaffold that was observed within a month might have promoted the local engraftment and survival of the cells.

In conclusion, we showed the feasibility to deliver MSCs to injured rat myocardium using a polysaccharide porous scaffold that improved engraftment in comparison with the most currently used approach of EC injection. Refinements of this approach, such as using injectable porous scaffolds containing appropriate molecules for cell differentiation or maintenance and sustained degradation profile may serve to enhance any benefits gained by cellular cardiomyoplasty.

ACKNOWLEDGMENTS

This work was supported by Inserm, Universities Paris 7 and Paris 13 and in part by Fondation de France, Fondation de l'Avenir (IM7-475) and grants from Agence Nationale de la Recherche (ANR-09-EBIO-001 3D and ANR-08-BIOT-012). Olivier Gournay was a recipient of « Société Française de Cardiologie ». We are grateful for the assistance of E. Balse (Inserm UMRS 956, Paris) for immunofluorescence staining, L. Louedec for animal care (Inserm U698, Paris) and F. Nadaud (UTC Compiègne, France) for ESEM images.

AUTHOR DISCLOSURE STATEMENT

No competing financial interests exist.

REFERENCES

1. Liu, J., Sluijter, J. P., Goumans, M. J., Smits, A. M., van der Spoel, T., Nathoe, H., and Doevendans, P. A. Cell therapy for myocardial regeneration. Curr Mol Med 9, 287, 2009.

2. Psaltis, P. J., Zannettino, A. C., Worthley, S. G., and Gronthos, S. Concise review: mesenchymal stromal cells: potential for cardiovascular repair. Stem Cells 26, 2201, 2008.

3. Fukushima, S., Varela-Carver, A., Coppen, S. R., Yamahara, K., Felkin, L. E., Lee, J., Barton, P. J., Terracciano, C. M., Yacoub, M. H., and Suzuki, K. Direct intramyocardial but not intracoronary injection of bone marrow cells induces ventricular arrhythmias in a rat chronic ischemic heart failure model. Circulation 115, 2254, 2007.

4. Freyman, T., Polin, G., Osman, H., Crary, J., Lu, M., Cheng, L., Palasis, M., and Wilensky, R. L. A quantitative, randomized study evaluating three methods of mesenchymal stem cell delivery following myocardial infarction. Eur Heart J 27, 1114, 2006.

5. Perin, E. C., Silva, G. V., Assad, J. A., Vela, D., Buja, L. M., Sousa, A. L., Litovsky, S., Lin, J., Vaughn, W. K., Coulter, S., Fernandes, M. R., and Willerson, J. T. Comparison of intracoronary and transendocardial delivery of allogeneic mesenchymal cells in a canine model of acute myocardial infarction. J Mol Cell Cardiol 44, 486, 2008.

6. Mooney, D. J., and Vandenburgh, H. Cell delivery mechanisms for tissue repair. Cell Stem Cell 2, 205, 2008.

7. Soto-Gutierrez, A., Yagi, H., Uygun, B. E., Navarro-Alvarez, N., Uygun, K., Kobayashi, N., Yang, Y. G., and Yarmush, M. L. Cell delivery: from cell transplantation to organ engineering. Cell Transplant 19, 655, 2010.

8. Chaouat, M., Le Visage, C., Autissier, A., Chaubet, F., and Letourneur, D. The evaluation of a small-diameter polysaccharide-based arterial graft in rats. Biomaterials 27, 5546, 2006.

9. Geckil, H., Xu, F., Zhang, X., Moon, S., and Demirci, U. Engineering hydrogels as extracellular matrix mimics. Nanomedicine (Lond) 5, 469, 2010.

10. Doucet, C., Ernou, I., Zhang, Y., Llense, J. R., Begot, L., Holy, X., and Lataillade, J. J. Platelet lysates promote mesenchymal stem cell expansion: a safety substitute for animal serum in cell-based therapy applications. J Cell Physiol 205, 228, 2005.

11. Poirier-Quinot, M., Frasca, G., Wilhelm, C., Luciani, N., Ginefri, J. C., Darrasse, L., Letourneur, D., Le Visage, C., and Gazeau, F. High resolution 1.5T magnetic resonance imaging for tissue engineering constructs: a non invasive tool to assess 3D scaffold architecture and cell seeding. Tissue Eng Part C Methods 16, 185, 2010.

12. Autissier, A., Le Visage, C., Pouzet, C., Chaubet, F., and Letourneur, D. Fabrication of porous polysaccharide-based scaffolds using a combined freeze-drying/cross-linking process. Acta Biomater 6, 3640, 2010.

13. Pfaffl, M. W. A new mathematical model for relative quantification in real-time RT-PCR. Nucleic Acids Res 29, 45, 2001.

14. Zimmermann, W. H., and Eschenhagen, T. Embryonic stem cells for cardiac muscle engineering. Trends Cardiovasc Med 17, 134, 2007.

15. Li, S. C., Wang, L., Jiang, H., Acevedo, J., Chang, A. C., and Loudon, W. G. Stem cell engineering for treatment of heart diseases: potentials and challenges. Cell Biol Int 33, 255, 2009.

16. Sun, J., Li, S. H., Liu, S. M., Wu, J., Weisel, R. D., Zhuo, Y. F., Yau, T. M., Li, R. K., and Fazel, S. S. Improvement in cardiac function after bone marrow cell thearpy is associated with an increase in myocardial inflammation. Am J Physiol Heart Circ Physiol 296, H43, 2009.

17. Li, Z., and Guan, J. Hydrogels for Cardiac Tissue Engineering. Polymers 3, 740, 2011.

18. Rosenzweig, M., Connole, M., Glickman, R., Yue, S. P., Noren, B., DeMaria, M., and Johnson, R. P. Induction of cytotoxic T lymphocyte and antibody responses to enhanced green fluorescent protein following transplantation of transduced CD34(+) hematopoietic cells. Blood 97, 1951, 2001.

19. Pfeifer, A., Ikawa, M., Dayn, Y., and Verma, I. M. Transgenesis by lentiviral vectors: lack of gene silencing in mammalian embryonic stem cells and preimplantation embryos. Proc Natl Acad Sci U S A 99, 2140, 2002.

20. Pouzet, B., Vilquin, J. T., Hagege, A. A., Scorsin, M., Messas, E., Fiszman, M., Schwartz, K., and Menasche, P. Factors affecting functional outcome after autologous skeletal myoblast transplantation. Ann Thorac Surg 71, 844, 2001.

21. Schuleri, K. H., Feigenbaum, G. S., Centola, M., Weiss, E. S., Zimmet, J. M., Turney, J., Kellner, J., Zviman, M. M., Hatzistergos, K. E., Detrick, B., Conte, J. V., McNiece, I., Steenbergen, C., Lardo,

A. C., and Hare, J. M. Autologous mesenchymal stem cells produce reverse remodelling in chronic ischaemic cardiomyopathy. Eur Heart J 30, 2722, 2009.

22. Muralidharan, S., Gu, J., Laub, G. W., Cichon, R., Daloisio, C., and McGrath, L. B. A new biological membrane for pericardial closure. J Biomed Mater Res 25, 1201, 1991.

23. Ozeren, M., Han, U., Mavioglu, I., Simsek, E., Soyal, M. F., Guler, G., and Yucel, E. Consequences of PTFE membrane used for prevention of re-entry injuries in rheumatic valve disease. Cardiovasc Surg 10, 489, 2002.

24. Shimizu, T., Yamato, M., Kikuchi, A., and Okano, T. Cell sheet engineering for myocardial tissue reconstruction. Biomaterials 24, 2309, 2003.

25. Wei, H. J., Chen, C. H., Lee, W. Y., Chiu, I., Hwang, S. M., Lin, W. W., Huang, C. C., Yeh, Y. C., Chang, Y., and Sung, H. W. Bioengineered cardiac patch constructed from multilayered mesenchymal stem cells for myocardial repair. Biomaterials 29, 3547, 2008.

26. Hamdi, H., Furuta, A., Bellamy, V., Bel, A., Puymirat, E., Peyrard, S., Agbulut, O., and Menasche, P. Cell delivery: intramyocardial injections or epicardial deposition? A head-to-head comparison. Ann Thorac Surg 87, 1196, 2009.

27. Simpson, D., Liu, H., Fan, T. H., Nerem, R., and Dudley, S. C., Jr. A tissue engineering approach to progenitor cell delivery results in significant cell engraftment and improved myocardial remodeling. Stem Cells 25, 2350, 2007.

28. Shi, C., Li, Q., Zhao, Y., Chen, W., Chen, B., Xiao, Z., Lin, H., Nie, L., Wang, D., and Dai, J. Stem-cell-capturing collagen scaffold promotes cardiac tissue regeneration. Biomaterials In Press, 2011.

29. Kraehenbuehl, T. P., Ferreira, L. S., Hayward, A. M., Nahrendorf, M., van der Vlies, A. J., Vasile, E., Weissleder, R., Langer, R., and Hubbell, J. A. Human embryonic stem cell-derived microvascular grafts for cardiac tissue preservation after myocardial infarction. Biomaterials 32, 1102, 2011.

30. Tan, M. Y., Zhi, W., Wei, R. Q., Huang, Y. C., Zhou, K. P., Tan, B., Deng, L., Luo, J. C., Li, X. Q., Xie, H. Q., and Yang, Z. M. Repair of infarcted myocardium using mesenchymal stem cell seeded small intestinal submucosa in rabbits. Biomaterials 30, 3234, 2009.

31. Leor, J., Aboulafia-Etzion, S., Dar, A., Shapiro, L., Barbash, I. M., Battler, A., Granot, Y., and Cohen, S. Bioengineered cardiac grafts: A new approach to repair the infarcted myocardium? Circulation 102, III56, 2000.

32. Chavan, V., Patil, N., and Karnik, N. D. Study of leukocytic hydrolytic enzymes in patients with acute stage of coronary heart disease. Indian J Med Sci 61, 73, 2007.

TABLES

Table 1: GFP^+ cells in rat myocardium were analyzed by real-time RT-PCR one and two months after *in vivo* administration with endocardial injection (EC) or implantation of cellularized scaffold. Results were expressed as a median value of GFP^+ cells (with range) and as a percentage of engraftment (n=5 per condition). No significant difference was observed between groups.

	1 month		2 months	
	EC	Scaffold	EC	Scaffold
Residual cell number	50 800 (10700-61600)	97 300 (12300-167200)	61 300 (12400-87400)	163 200 (17500-2213000)

FIGURES CAPTION

Figure 1: Polysaccharide-based scaffold.

Macroscopic view of a dried porous scaffold (A, 6 mm diameter, 1 mm thickness). Porosity was evidenced with Environmental Scanning Electron Microscopy (B, scale bar 200 μm) and confocal microscopy observation of fluorescent FITC-dextran scaffold (C, scale bar 200 μm). Absorbance of MTT assay performed at day 1 after seeding rat bone marrow derived mesenchymal stem cells on porous scaffold as a function of the initial cell number. Non-cellularized porous scaffolds were used as blanks. Results are expressed as the mean value of the absorbance data +/- SEM (n=3). (D). Cells were observed as clusters in scaffold pores with light microscopy (E, 10x magnification). Cell viability within scaffold was confirmed with a live & dead assay. Bright green live cells were observed with a confocal microscope, whereas only few dead cells with compromised membranes fluoresce in red (F, scale bar 20μm).

Figure 2: Implantation of scaffolds on rat heart.

One month after implantation, scaffold on normal cardiac tissue was found intact (A, scaffold was stained with alcian blue for imaging purposes, scale bar: 2mm), as confirmed by fluorescent microscopic observation of heart sections showing cardiac tissue green autofluorescence and FITC-labelled scaffold (B, scale bar 100 μm). In contrast, no scaffold could be identified macroscopically on infarcted cardiac tissue after one month (C, scale bar: 2mm) and only remnants of the FITC-scaffold were seen embedded or integrated into the adjacent tissue on heart sections (D, scale bar 100 μm).

Figure 3: Cell transfer into myocardium.

MSCs were characterized by their spindle shaped morphology, scale bar: 20 μm (A) together with the expression of CD90, CD29 and CD106 and lack of CD45 (B) and their capacity to differentiate (C) into osteogenic (top), chondrogenic (middle), and adipogenic (bottom) cell lineages (left, without induction; right, with induction).[10] MSCs were lentivirally infected using a dual-promoter that

included GFP and PAC and transduced cells preserved their spindle-shaped morphology. scale bar: 40 µm (D). Fluorescence emitted by a defined number of GFP^+cells was used as calibrator for quantification of residual GFP^+ cells in myocardium (E).

Figure 4: Cell localization in infarcted area.

Microscopic observation of green autofluorescent cardiac tissue (A) containing double-labelled PKH/BrdU cells one month after implantation of scaffold loaded with cells (scale bar : 1mm). (B) is a magnification of the infarcted area highlighted in A. Red PKH-labelled cells (C, scale bar : 1mm and D, scale bar : 50 µm) and BrdU-labelled cells were identified in the same area (D, with DAB staining, scale bar : 100 µm). GFP^+ cells were identified in cardiac tissue 2 months after implantation of scaffold loaded with cells. Indirect immunohistofluorescence was performed with both Alexa 488-anti-GFP and Alexa 594-anti-sarcomeric alpha-actinin (E). Original magnification 10x.

Figure 5: Histology and RT-PCR analysis.

(A) Typical appearance of the left ventricular scarred area. Haematoxylin/eosin (top row) and sirius red (bottom row) stained sections of heart tissue 2 months after implantation of scaffold loaded with cells (left column) or direct injection of cell suspension (right column). Scale bar 1 mm. (B) Fibrosis area was quantified by histomorphometric measurement on Sirius red stained sections and results are expressed as mean ± SEM (n=2 measurements for 3 animals in each group). (C) mRNA expression levels of matrix metalloproteases MMP-2, MMP-9 and vascular endothelial growth factor (VEGF) into myocardium were analyzed by real-time RT-PCR. Transcription factors mRNA levels, normalized against HPRT, UBC and Ywhaz as reference genes, were expressed as relative unit of averaged mRNA levels in myocardium of a control animal subjected to myocardial infarct but without cell administration. No effect was obtained with MMP-2 and MMP-9, but a significant increase of mRNA level for VEGF was observed at 2 months with the cellularized scaffold. *indicates a significant difference ($p<0.05$)

Figure 6: Functional assessment by echocardiography.

Echocardiography was performed at 7 days and 2 months after myocardial infarction and results are presented as a percentage of day 7 value for animals having received either a control scaffold without cells, endocardial injection or a cellularized scaffold (n=9). LVFS: left ventricular fractional shortening (A); LVESD: left ventricular end systolic diameter (B). No significant difference was observed between groups.

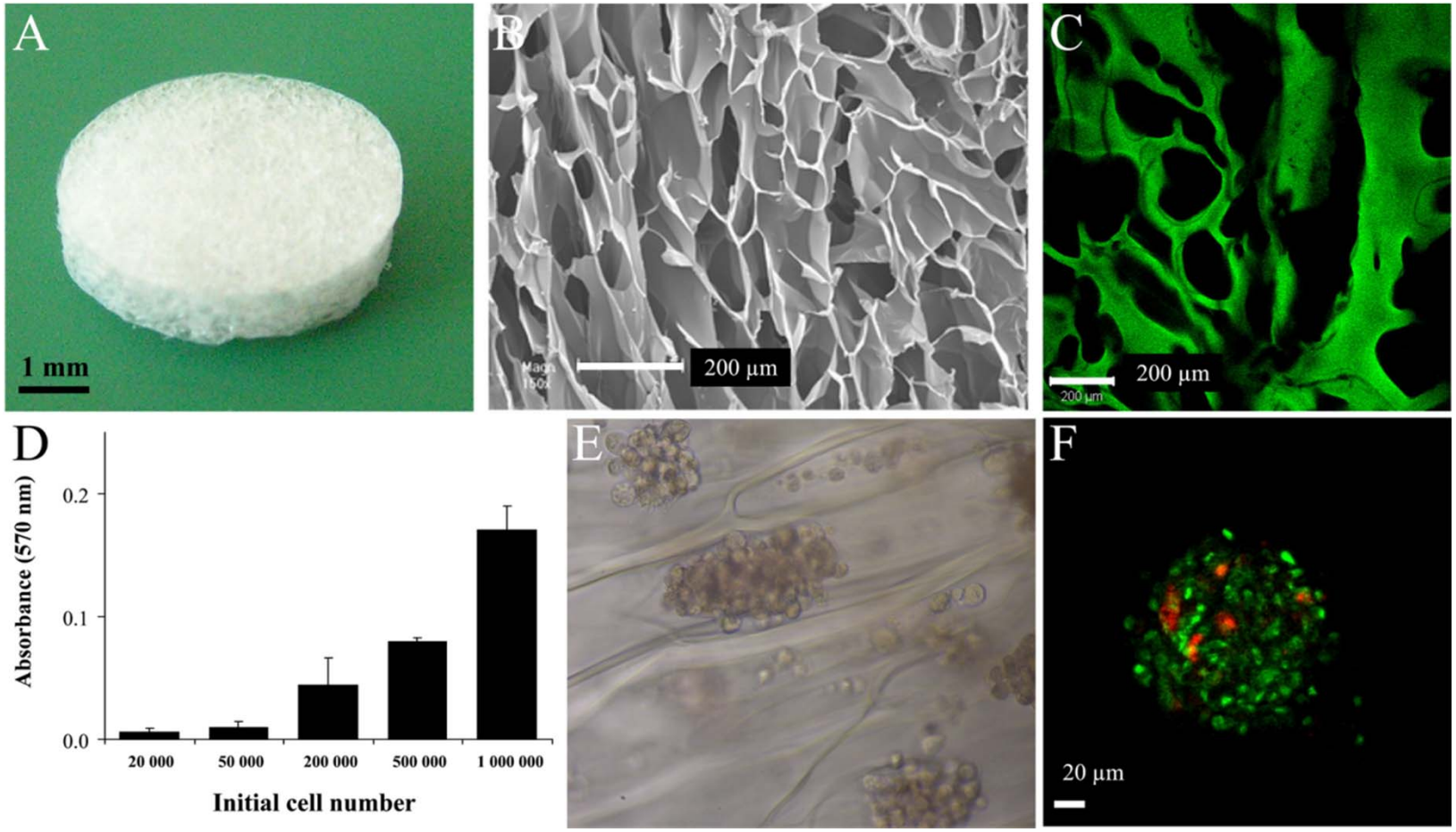
A
1 mm
B
200 µm
C
200 µm
D
Absorbance (570 nm)
0.2
0.1
0.0
20 000
50 000
200 000
500 000
1 000 000
Initial cell number
E
F
20 µm

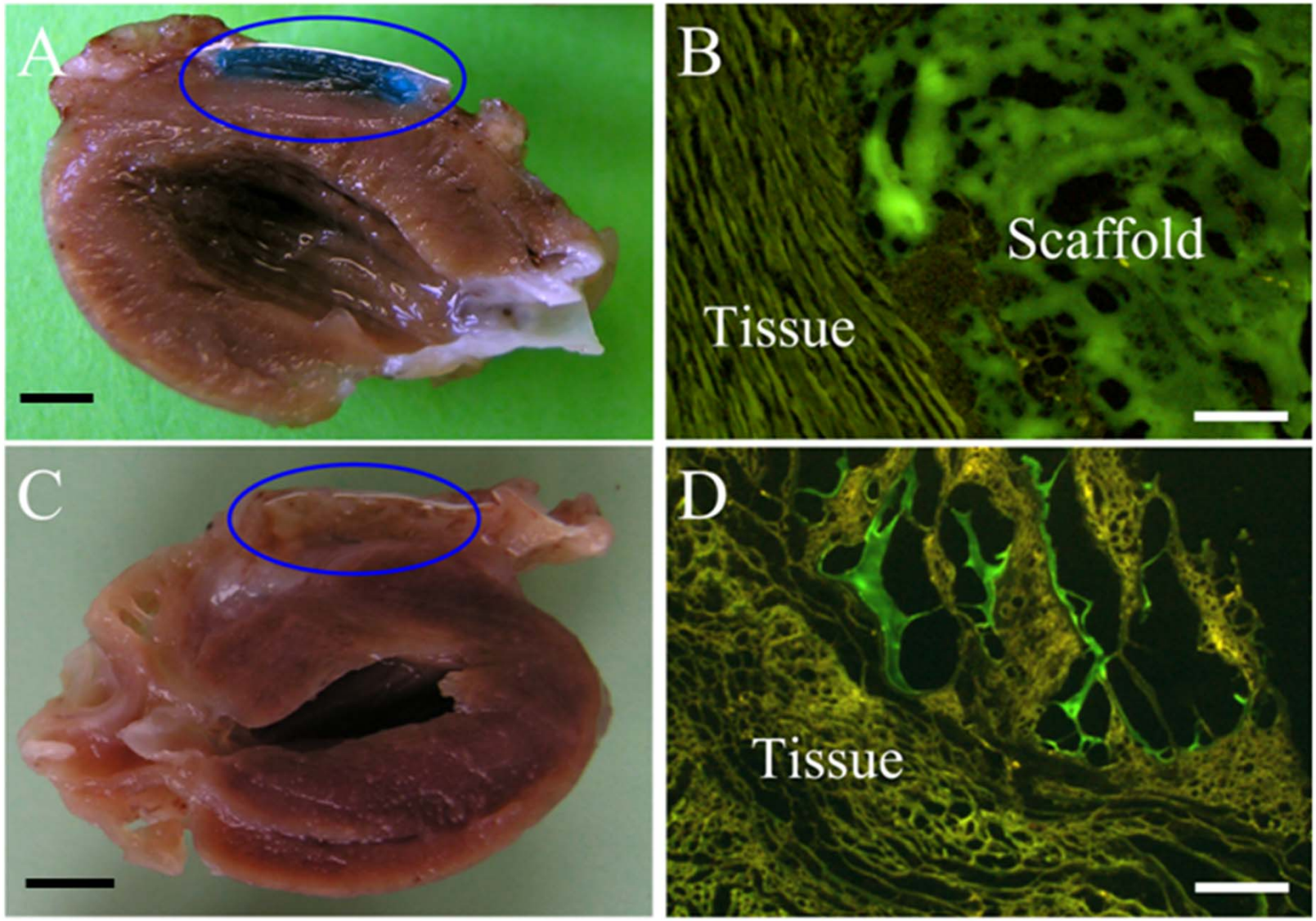
A
B
Scaffold
Tissue
C
D
Tissue

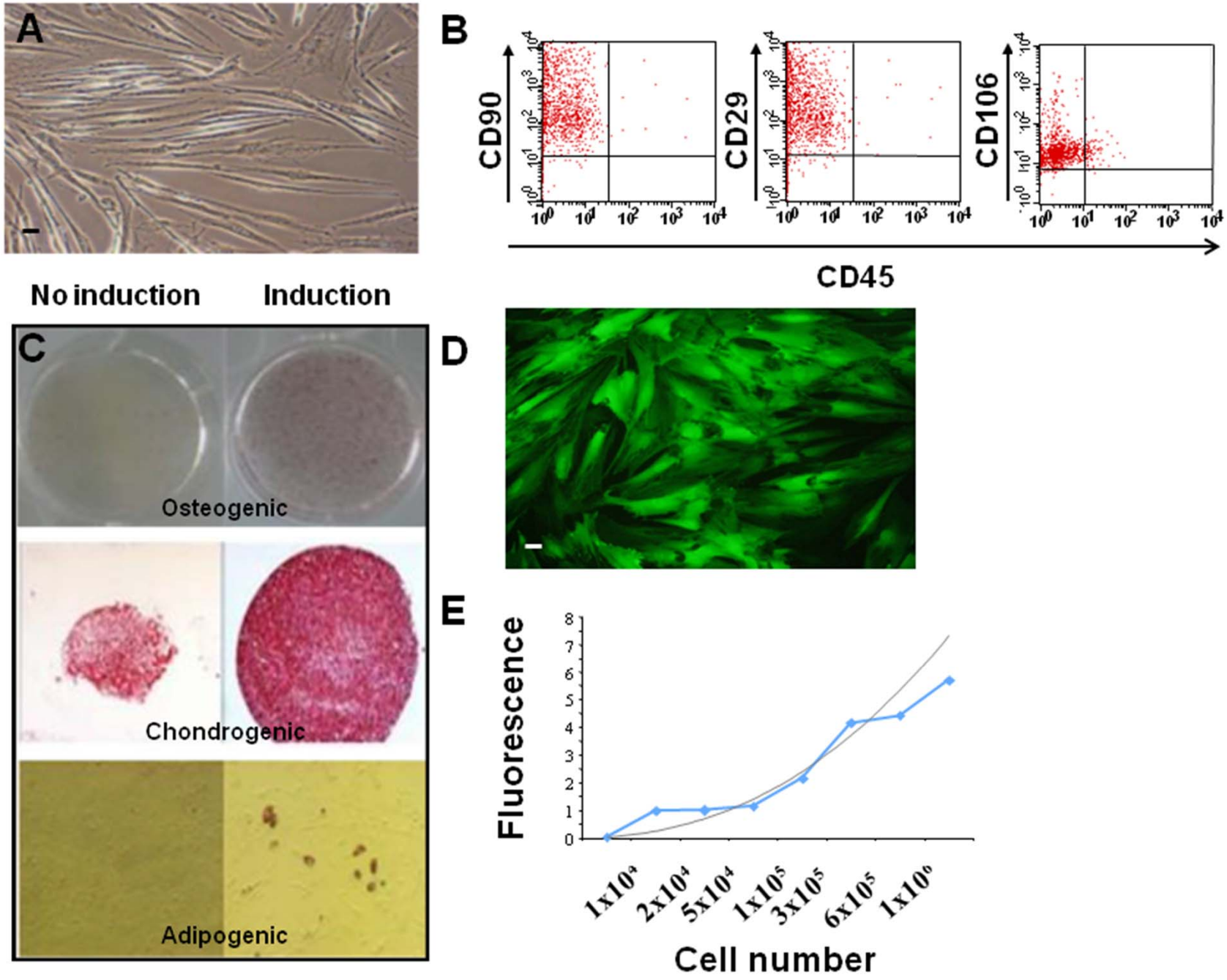
A
B
CD90
CD29
CD106
CD45
No induction
Induction
C
Osteogenic
Chondrogenic
Adipogenic
D
E
Fluorescence
Cell number
1x10³
2x10⁴
5x10⁴
1x10⁵
3x10⁵
6x10⁵
1x10⁶

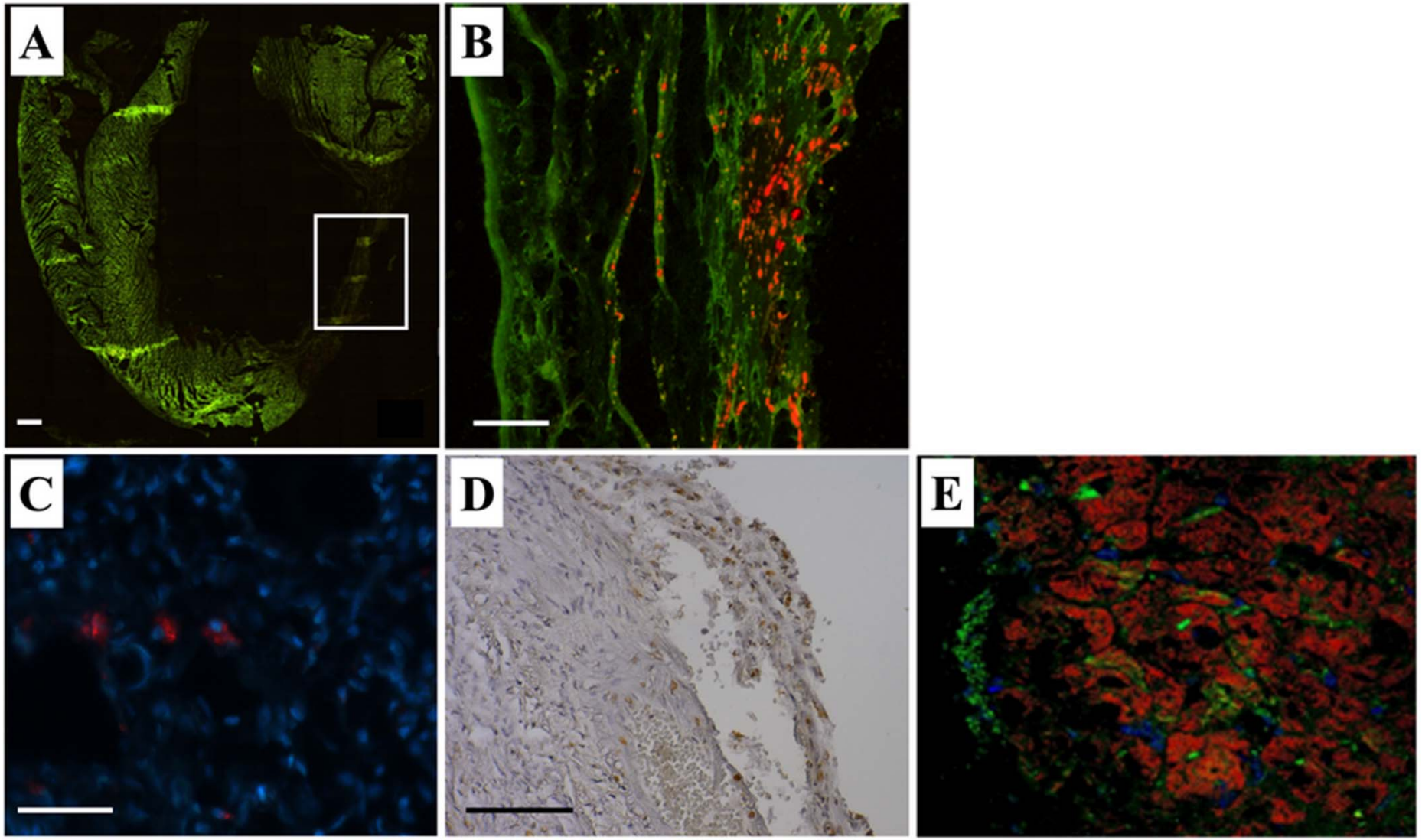
A
B
C
D
E

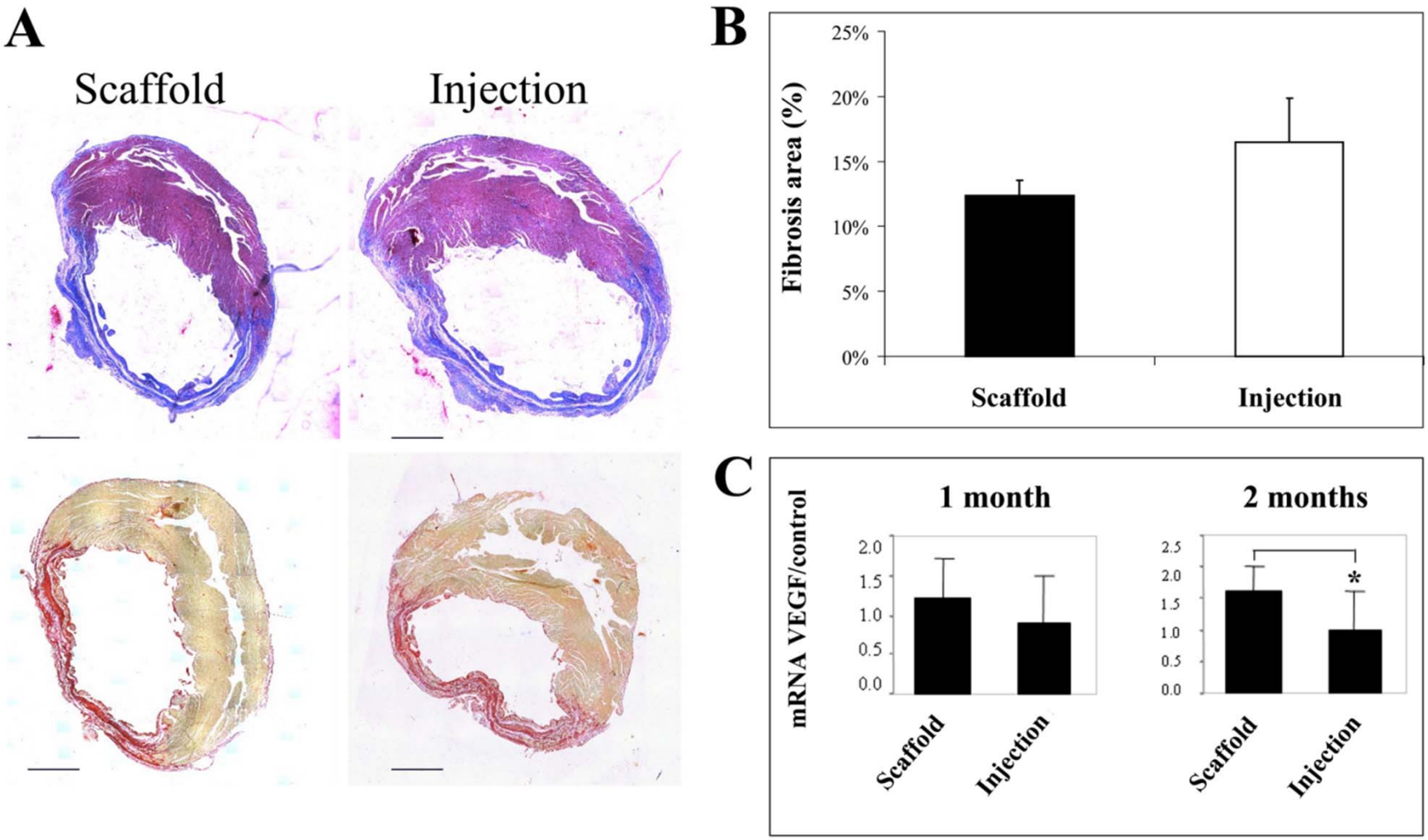
A
Scaffold
Injection
B
Fibrosis area (%)
25%
20%
15%
10%
5%
0%
Scaffold
Injection
C
mRNA VEGF/control
1 month
2 months
2.0
1.5
1.0
0.5
0.0
2.5
2.0
1.5
1.0
0.5
0.0
*
Scaffold
Injection
Scaffold
Injection

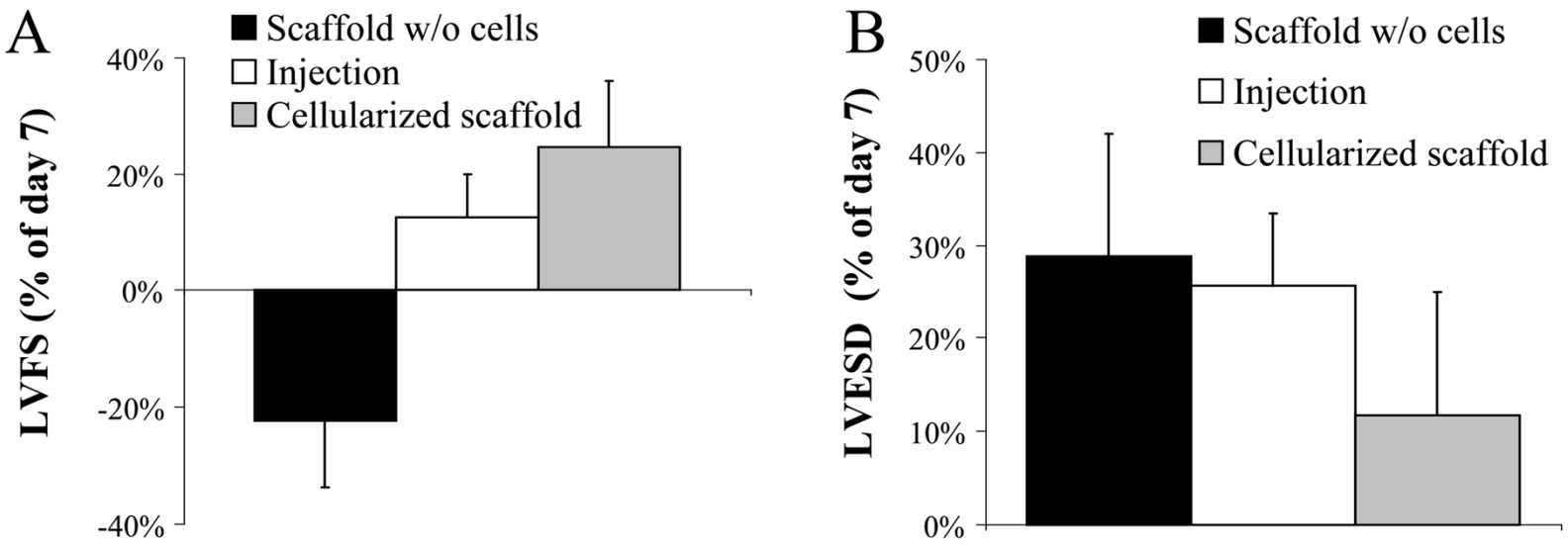
A
LVFS (% of day 7)
40%
20%
0%
-20%
-40%
Scaffold w/o cells
Injection
Cellularized scaffold
B
LVESD (% of day 7)
50%
40%
30%
20%
10%
0%
Scaffold w/o cells
Injection
Cellularized scaffold